

Applications of Responsive Small Satellites with MIT TILE Electrospray Propulsion

Ciara McGrath and Malcolm Macdonald
University of Strathclyde, Glasgow, United Kingdom, G1 1XJ

Paulo Lozano, David Miller and David Krejci
Massachusetts Institute of Technology, Cambridge, MA, USA, 02139

Responsive, manoeuvrable small satellites are an enabling technology for affordable, flexible and agile space missions with possible applications as wide-reaching as military reconnaissance, disaster response, and even wildlife tracking. This paper presents an analysis of some of these applications and is the outcome of a four month collaborative research visit at the Space Propulsion Laboratory of the Massachusetts Institute of Technology. This work builds upon the analytical satellite manoeuvring strategy previously developed by the author, and analyses the potential capabilities and applications of small satellites equipped with the MIT TILE electrospray thruster. This previously developed analytical method enables the rapid investigation of the manoeuvres of a constellation of small satellites, with the goal of targeting a particular region on the Earth. A full overview of the solution space can be rapidly generated, allowing for the mission designer or operator to trade off all possible manoeuvres and select the best solution for their specific purpose. The MIT TILE is a modular, miniaturised MEMS based propulsion system for nanosatellites capable of producing $350\mu\text{N}$ nominal thrust for up to 200hrs operation. A standard TILE system weighs $<450\text{g}$ and is sized to fit in 0.5U of a CubeSat. Three case studies are presented which demonstrate the effectiveness of responsive satellites in disaster response missions. The first case study considers a rapid flyover of Los Angeles following an earthquake. The results show a reduction in flyover time of almost 9 days using $21\text{m/s } \Delta V$ when compared with a non-manoevring satellite. A second case study considers a fire detection constellation of 24 satellites, which can manoeuvre to provide targeted coverage of a given region as required. Selecting the Cairngorms National Park in Scotland, UK as the region of interest, the results show that by manoeuvring the constellation to directly target the region, an increase in coverage is achievable over the entire target area, with total coverage times of some areas more than doubled from 3.4 minutes coverage in a week to 8.4 minutes. The final case study considers providing communication services to helicopters at a range of locations from the UK to Svalbard, Norway. The manoeuvring capabilities of the satellites are used to follow the helicopters over an eight week period. Results show that a single satellite using $<150\text{m/s } \Delta V$ can achieve 50 flyovers of the helicopters during the journey, compared with 24 flyovers if a static satellite is used. These missions are all shown to be possible with existing technologies, and they exemplify the dramatic improvement in performance that can be achieved by using manoeuvrable satellites.

Nomenclature

a	=	semi-major axis
a_0	=	semi-major axis at manoeuvre start
a_3	=	semi-major axis at manoeuvre end
d	=	haversine distance between point of interest and sub-satellite point
i	=	inclination
t	=	time
t_0	=	time at epoch
t_{total}	=	total time required for the manoeuvre
u	=	argument of latitude
u_0	=	argument of latitude at epoch
A	=	constant acceleration applied by the propulsion system
J_2	=	coefficient of the Earth's gravitational zonal harmonic of the 2 nd degree
R_e	=	mean Earth radius
δ_{ssp}	=	latitude of sub-satellite point
δ_{POI}	=	latitude of point of interest
μ	=	standard gravitational parameter of Earth
ω_e	=	angular velocity of Earth

ΔV_{total}	=	total change in velocity required for manoeuvre
Ψ_{ssp}	=	longitude of sub-satellite point
Ψ_{POI}	=	longitude of point of interest
Ω	=	right ascension of the ascending node
Ω_{total}	=	total change in right ascension of the ascending node
Ω_0	=	right ascension of the ascending node at epoch
Ω_{et0}	=	right ascension of Greenwich at epoch

I. Introduction

NANO-SATELLITES, defined as those satellites with a mass of 1-10kg, are becoming increasingly popular amongst academic, governmental and commercial organisations [1-4]. The global adoption of the CubeSat standard has fuelled this development, as standardised sub-system, spacecraft bus, and launch system adapters continue to reduce mission costs and improve accessibility to space hardware [5]. This interest has spurred research into the design and development of communications systems, on-board computers, power supply units and propulsion systems specifically for small spacecraft. These miniaturised technologies have increased the capabilities of nano-satellites in recent years, to the point where they are now capable of delivering truly valuable science and Earth observation data.

The low cost and short development time associated with small satellites makes them ideal for missions requiring large numbers of satellites, short design cycles, or high risk missions where the chance of loss of the satellite is high. One such application is responsive satellite constellations which are capable of manoeuvring in response to a real-time change in mission requirements. Such a mission would allow previously impossible flexibility in mission design and operation by allowing the user to actively change the mission goals, and the constellation architecture, throughout the mission life. It could also further reduce mission design time by allowing for uncertainty of mission during the design phase, and instead allow the satellites to be designed for maximum flexibility. Such missions are of greatest benefit when multiple satellites are available for tasking, and the increased risk in operating a mission of this kind could be off-set through the use of low-cost small satellites.

An enabling technology for such a mission is a small, light-weight, highly efficient propulsion system, usable by nano-satellites, such as the electrospray propulsion system developed by the Space Propulsion Laboratory (SPL) at the Massachusetts Institute of Technology (MIT) [6]. Using a method previously developed at the University of Strathclyde, the manoeuvres of a satellite, or satellites, equipped with such a system can be analytically described and rapidly analysed [7-9]. This method provides an insight into the complete solution space of a given scenario, allowing the user to select the most suitable manoeuvre or series of manoeuvres for their purposes. This paper applies this technique to a variety of disaster response case studies to demonstrate the improvement in performance that could be achieved using nano-satellites equipped with an electrospray propulsion system, such as that available from MIT. This system is fully developed, tested and flight ready in its current state, with significant performance improvements expected in the coming years.

II. Overview of MIT TILE

The Space Propulsion Laboratory at the Massachusetts Institute of Technology has developed highly miniaturized electrospray thrusters with thrust densities comparable to large electric propulsion devices [10-12]. The propellant used is an ionic liquid, composed of positive and negative charges, much like a “plasma in a bottle”. This propellant is fed passively, by capillary forces, from a tank to an array of sharp emitter structures. When applying a potential difference between the liquid and a counter-electrode, electrostatic pull is counteracted by surface tension, forming a so-called “Taylor cone”. When surpassing a certain potential threshold, ions are extracted from the cone’s tip. These ions are then accelerated by the applied potential to high exhaust velocities, producing thrust at highly efficient propellant utilization.

To increase emission current, and therefore total thrust, emission sites can be multiplexed at the device level by building large arrays of emitting structures, and additionally at the system level by operating multiple arrays in parallel. Such emitter arrays operated in parallel can share tank structures, forming clusters of emitters. The proposed tile system is shown in **Figure 1** featuring a total of 32 electrospray emitter arrays, partially sharing propellant tanks. This design allows for large ΔV in the main propulsion direction, and is also capable of thrust vectoring by firing individual thrusters, as well as thrusting along the rotational axis using four dedicated roll thrusters. While the propellant mass can be varied by adjusting the tank height of the system, the design shown in **Figure 1** allows for >90g of propellant, corresponding to an operation time of up to 200 hours at the nominal thrust of 350 μ N. For a 3U CubeSat, weighing 3kg, this corresponds to a total available ΔV of 120m/s.

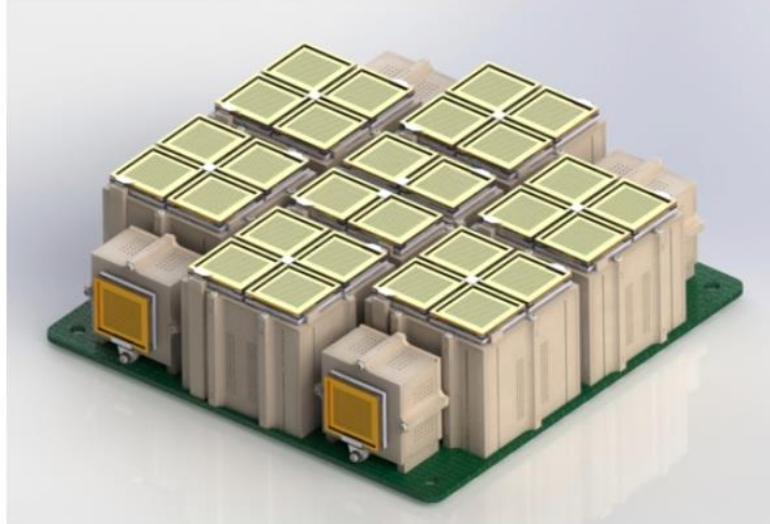


Figure 1: Computer Aided Drawing of the TILE propulsion system [13].

III. Method

This work demonstrates the capabilities of a small satellite, and small satellite constellations, equipped with the MIT TILE thruster to respond to rapid changes in mission requirements. Due to the limited propellant available on board small spacecraft, only in-plane, low-thrust manoeuvres are considered. These manoeuvres can only directly change the altitude of the satellite, but, by considering the natural perturbing force of the Earth's J_2 effect, controlled changes in the other orbit elements can be achieved.

The manoeuvre strategy used in this paper is a so-called 3-Phase Manoeuvre. In this case, the satellite raises or lowers its altitude in Phase 1, it drifts at this new altitude in Phase 2, and in Phase 3 the satellite manoeuvres once again to achieve the desired final altitude. This is illustrated in **Figure 2**. Previous work by the author has developed an analytical expression to identify the location of the spacecraft sub-satellite point after such a manoeuvre has been carried out. This expression is derived from the Gauss-Lagrange planetary equations and assumes a circular orbit, with the only perturbing forces those of the J_2 effect and the satellite's propulsion system. The derivation of this analytical solution is well documented and validated against numerical simulations [7-9].

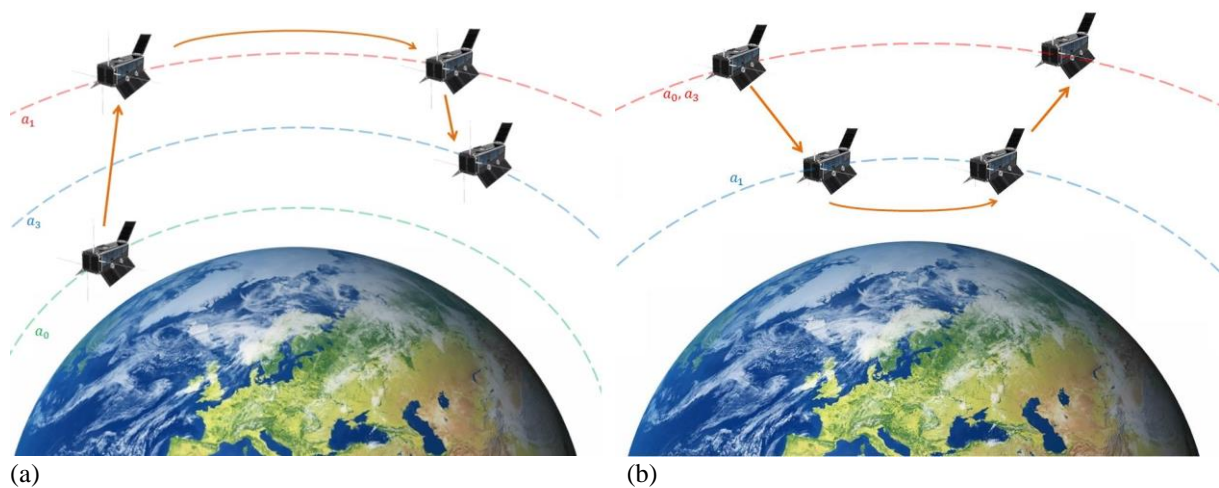


Figure 2: (a) General 3-Phase manoeuvre and (b) 3-Phase manoeuvre returning to initial altitude. Initial orbit (a_0), intermediate orbit (a_1) and final orbit (a_3) are marked by dashed lines.

The result of the method is two analytical expressions for the change in Right Ascension of the Ascending Node (RAAN) and Argument of Latitude (AoL) of the satellite post-manoeuvre. This expression can then be linked to the geocentric latitude and longitude of the spacecraft sub-satellite point (SSP) using spherical geometry. The result is two analytical equations which give the geocentric latitude and longitude of the sub-satellite point as a function of the satellite initial conditions and the time and change in velocity (ΔV) required for the manoeuvre. That is,

$$\delta_{ssp} = f(J_2, R_e, \mu, i, a_0, a_3, u_0, A, \Delta V_{total}, t_{total}) \quad (1)$$

and

$$\Psi_{ssp} = f(J_2, R_e, \mu, \omega_e, i, a_0, a_3, u_0, \Omega_0, t_0, \Omega_{et0}, A, \Delta V_{total}, t_{total}) \quad (2)$$

where δ_{ssp} is the geocentric latitude of the sub-satellite point, Ψ_{ssp} is the geocentric longitude of the sub-satellite point, and all other variables are as defined in the nomenclature.

If the latitude and longitude of a target point-of-interest (POI) is known, then the distance between the POI and the SSP can be calculated post-manoeuvre using the haversine formula given by

$$d = 2R_e \sin^{-1} \left[\sqrt{\sin^2 \left(\frac{\delta_{ssp} - \delta_{POI}}{2} \right) + \cos(\delta_{ssp}) \cos(\delta_{POI}) \sin^2 \left(\frac{\Psi_{ssp} - \Psi_{POI}}{2} \right)} \right] \quad (3)$$

which gives the curved distance between two points on the Earth's surface. This allows the distance between the POI and the satellite SSP after a manoeuvre to be directly calculated as a function of the time required for the manoeuvre and the ΔV required using a single analytical expression. It is of note that this analytical solution is derived from the Gauss-Lagrange Variation of Parameters (VOP) equations, and as such the mean values for the orbital elements should be used for consistency with the underlying theory [14].

IV. Rapid Flyover Mission Case Study: Earthquake in Los Angeles

The first case study considered is a rapid flyover mission, such as might be desired following a disaster. For this example, a powerful earthquake is conceived to have occurred in Los Angeles, USA. Up to date Earth observation data is requested to support the response teams. The satellite selected to provide the response in this case is assumed to be in the same orbit as the International Space Station (ISS) whose orbit parameters are given in **Table 2**. The orbital constants used for the analysis are in **Table 1**. The satellite propulsion system acceleration is calculated assuming a 3kg satellite (e.g. a 3U CubeSat), equipped with the MIT TILE electrospray propulsion system which is capable of producing 350 μ N of nominal thrust as described in Section II. The goal of the mission is to reduce the revisit time of the satellite over Los Angeles, California, to provide up-to-date imagery as soon as possible after the disaster.

A. Non-manoeuving satellite

Considering first a non-manoeuving satellite in the specified orbit, the distance between the spacecraft SSP and Los Angeles is plotted in **Figure 3** over a 16 day period as calculated by the analytical method described in Section III. The orange horizontal line is drawn at half the swath width, indicating the distance at which Los Angeles will be visible to the satellite. The red dots mark the four instances over the 16 day period at which Los Angeles will be in view of the satellite. The times of each of these target fly-overs and the distance of the SSP from the Los Angeles at this time are given in **Table 3**. In this case there is a 12.5 day gap between flyover two and three, during which time no satellite data can be collected over Los Angeles.

Parameter	Symbol	Value	Units
Gravitational Parameter	μ	3.986×10^{14}	m^3/s^2
Radius of Earth	R_e	6.371×10^3	km
J_2 Parameter	J_2	1.0827×10^{-3}	-
Angular velocity of Earth	ω_e	7.2921×10^{-5}	rad/s

Table 1: Orbital Constants.

Parameter	Symbol	Value	Units
Propulsion acceleration	A	$\pm 1.1667 \times 10^{-4}$	m/s^2
Inclination	i	51.64	deg
Initial semi-major axis	a_0	6773	km
Final semi-major axis	a_3	6773	km
Initial AoL	u_0	0	rad
Initial RAAN	Ω_0	0	rad
Latitude of POI	δ_{target}	34.05	deg
Longitude of POI	Ψ_{target}	-118.24	deg
Epoch	-	01 Jan 1990 00:00:00.0000	-
Right ascension of Greenwich at epoch	Ω_{et0}	100.38641	deg
Instrument swath width	S	200	km

Table 2: Rapid Flyover Mission Case Study Parameters.

Viewing Instance	Time from mission start, days	Distance from SSP to POI, km
1	0.136	20.52
2	1.433	55.24
3	13.912	86.98
4	15.209	52.84

Table 3: Fly-over times of Los Angeles for non-maneuvring satellite and corresponding distance to POI.

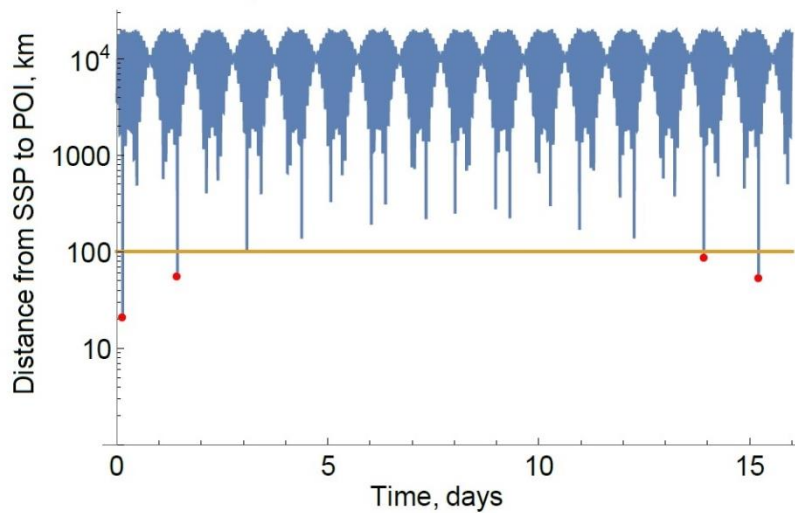


Figure 3: Fly-over times of Los Angeles for non-maneuvring satellite and corresponding distance to POI.

B. Manoeuvring satellite

The manoeuvring case considers a satellite in the same orbit as above, but equipped with the MIT TILE propulsion system capable of producing a total ΔV of 120m/s. The satellite is tasked to begin manoeuvring after the second flyover identified above at 1.433 days from mission start, with the aim of reducing the time to the next flyover from 12.5 days. The analytical method is used to identify the shortest flyovers possible using up to 120m/s ΔV . The results of this are presented in **Figure 4** where the flyover time is calculated for ΔV values ranging from 0m/s to 120m/s in 1m/s increments. Time here is measured from the beginning of the manoeuvre, that is, from viewing instance two. These results show that the minimum achievable flyover time for a $\Delta V < 120$ m/s is 3.623 days, or 86.96 hours, achieved with a ΔV of 36m/s. However, it is of note that a very similar time of flyover can be achieved using a lower ΔV . For example, a flyover time of 87.02 hours is achievable with 21m/s ΔV . This is clear from the solutions shown in **Figure 4**, however as the solution space is discontinuous such insights may be difficult to gain through numerical methods alone. For the case study being considered, the use of 21m/s ΔV gives an 87 hour manoeuvre time and a potential decrease in flyover time of almost 9 days when compared with the non-manoevring case.

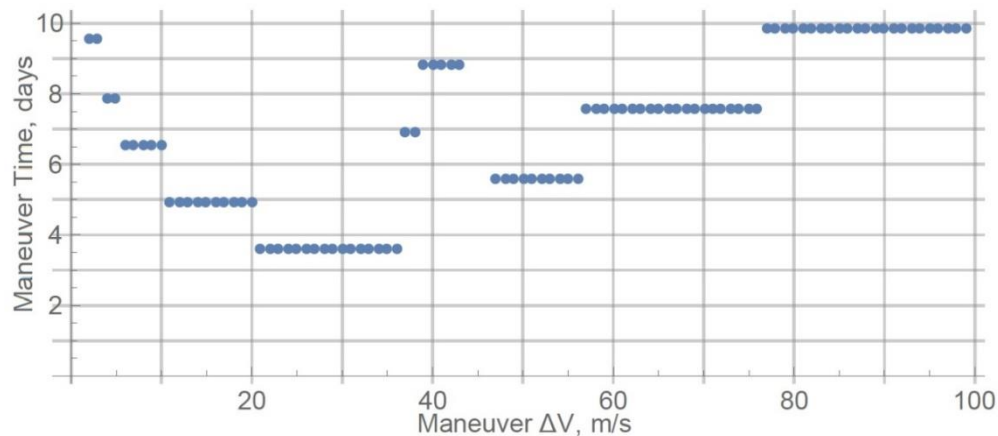


Figure 4: Manoeuvre time required to produce a pass over Los Angeles for a given ΔV .

V. Disaster Response Constellation Case Study: Forest Fire in Scotland

A. Introduction

The second case study considers a disaster response constellation, such as the nano-satellite constellation proposed by the Universitat Politècnica de Catalunya for global fire detection [15]. They identify a need for near real time, global fire monitoring capability and suggest a constellation of CubeSats equipped with a high resolution optical system to provide such a service. They state that a minimum 6 hour revisit time is required for all regions of interest, but a 1 hour revisit is desirable. To meet the minimum revisit time of 6 hours with a 50km instrument swath, they propose a 55° inclined orbit at 600km altitude with 4 orbit planes and 6 satellites per plane, for 24 total satellites. To meet the desired revisit time of 1 hour with a 50km instrument swath, they propose a 55° inclined orbit at 600km altitude with 5 orbit planes and 10 satellites per plane, for 50 total satellites. Both constellations are assumed to be non-manoevrable. A similar constellation is under development by the Spanish company AISTECH who envision a 100 nano-satellite constellation with the first due for launch in 2018 [16].

This case study aims to determine whether an improvement in performance could be achieved through the use of manoeuvrable satellites. For this analysis, the ReCon concept proposed by the Massachusetts Institute of Technology is used [17]. In this concept, the Earth observing constellation has two operational modes which it can manoeuvre between. The first mode is a global observation mode (GOM) in which the satellites are spread out to provide even coverage of the observation region. The second mode is regional observation mode (ROM) in which some of the satellites are moved into repeating ground track (RGT) orbits over a specific point of interest to provide improved coverage of the region. For the proposed fire monitoring mission, the constellation in GOM would be used to detect the outbreak of fire, and then would transition to ROM to provide more frequent revisits of the affected area. Once the fire has been dealt with, the constellation would return to GOM and continue global observations.

The constellation proposed for this case study is based on the minimum constellation proposed by the Universitat Politècnica de Catalunya for fire monitoring, but with an inclination of 60° to incorporate the UK wholly in the observable region. For an orbit inclined at 60° , a repeat ground track of 15 orbits per day requires an altitude of 513.087km as calculated for a circular orbit using the method described in [17] and [18]. With this in mind, the altitude of the GOM constellation is selected as 550km to reduce the required manoeuvre distance between GOM and ROM while still maintaining global coverage. The parameters of the constellation are given in **Table 4**. All orbits are assumed to be circular and the constants given in **Table 1** are used.

The case to be analysed is that of a forest fire in the Cairngorms National Park in Scotland, UK, which is shown in **Figure 5**. The area of interest is assumed to be a rectangle encompassing the park, with the parameters given in **Table 5**. In this case, it is assumed that a fire in the Cairngorms has been detected and the constellation will respond by manoeuvring two satellites per orbit plane into repeating ground tracks over the area, one which will view the area on an upwards pass and one which will view it on a downwards pass, to improve the revisit time and coverage available. It is assumed that these manoeuvres will begin at epoch.

Parameter	Value	Units
Number of orbit planes	4	-
Number of satellites per plane	6	-
Total number of satellites	24	-
Inclination	60	deg
GOM Altitude	550	km
ROM Altitude	513.087	km
RAAN spacing between orbit planes	90	deg
In plane spacing between satellites	60	deg
Instrument swath width	50	km
Propulsion acceleration	$\pm 1.1667 \times 10^{-4}$	m/s^2
Epoch	01 Jan 1990 00:00:00.0000	-
Right ascension of Greenwich at epoch	100.38641	deg

Table 4: Disaster Response Constellation Case Study Initial Constellation Parameters.

Parameter	Value	Units
Maximum latitude of POI	57.66	deg
Minimum latitude of POI	56.58	deg
Maximum longitude of POI	-2.65	deg
Minimum longitude of POI	-4.64	deg

Table 5: Cairngorms National Park Region of Interest.

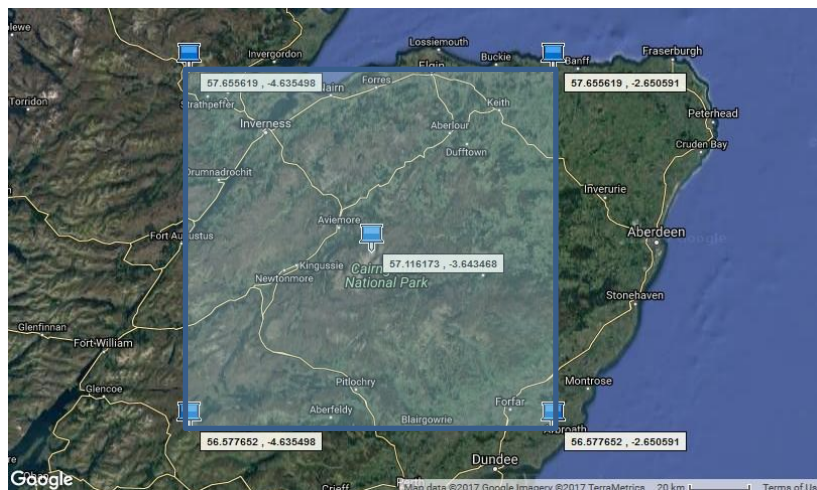


Figure 5: Cairngorms National Park Region of Interest [19].

B. Method

In order to decide which satellites should be manoeuvred, and what form these manoeuvres should take, each satellite is analysed using the analytical method described in Section III, producing a list of all possible manoeuvres that each satellite could perform which would conclude with the satellite over the Cairngorms and in a repeating ground track orbit. An example of these results are shown for two satellites in the same plane, Satellite 1 ($u_0 = 0^\circ, \Omega_0 = 0^\circ$) in **Figure 6** and Satellite 4: ($u_0 = 180^\circ, \Omega_0 = 0^\circ$) in **Figure 7**. Similar results are obtained for all 24 satellites. From these results it is clear that each possible manoeuvre will have a corresponding time and ΔV associated with it. It is also clear that although for all solutions shown the satellite SSP will pass within the region of interest, the distance from the SSP to the centre of the POI will vary. This full overview of the solution space allows the operator to identify all possible solutions and then select those which best meet their mission criteria, whether that be to minimise time to first viewing, minimise fuel usage, or, as is often the case, a compromise between the two.

Looking at Satellite 1 and Satellite 4 in particular, as shown in **Figure 6** and **Figure 7** respectively, it is clear that manoeuvring Satellite 4 is a much more attractive option. The minimum manoeuvre time for Satellite 1 is in excess of 8 days, and requires a minimum of 50m/s ΔV . Satellite 4 by comparison can complete the manoeuvre in as little as 2 days, with a ΔV of just 20m/s. Manually selecting the ‘best’ manoeuvre for each of the 24 satellites gives the results shown in **Table 6**. From this the highlighted satellites are selected to manoeuvre as they offered the best options to fill both slots in the RGT orbit with the minimum ΔV and manoeuvre time. From those satellites selected, Satellite 20 requires the longest manoeuvre time of 4.7 days. At this time, all other satellites will have finished manoeuvring and Satellite 20 will be positioned above the POI.

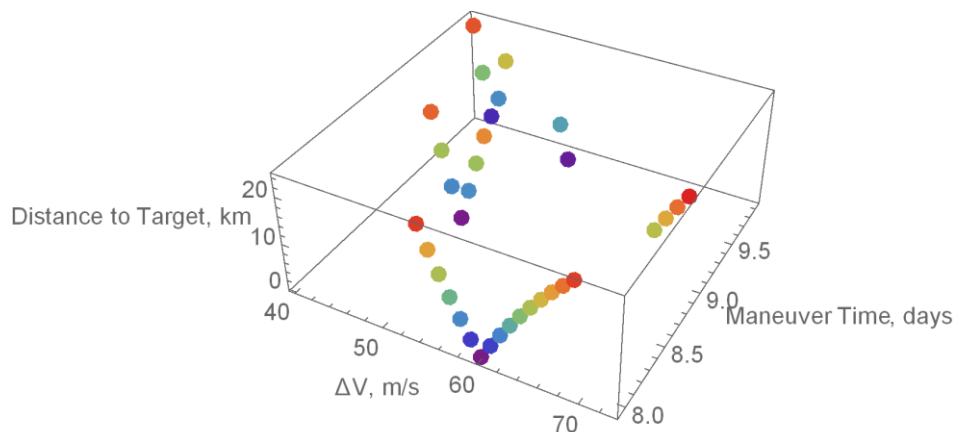


Figure 6: Satellite 1 - Possible flyovers of Cairngorms and corresponding manoeuvre time, ΔV and distance to target at closest pass.

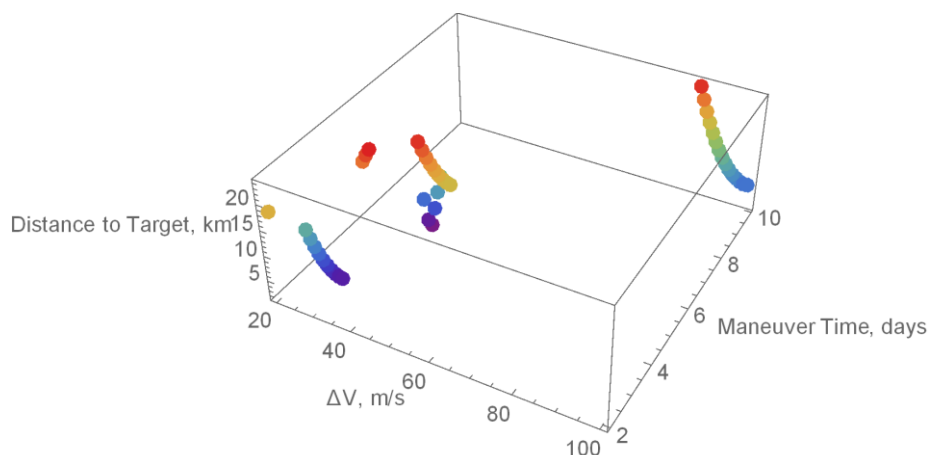


Figure 7: Satellite 4 - Possible flyovers of Cairngorms and corresponding manoeuvre time, ΔV and distance to target at closest pass.

C. Results

To analyse the results, the coverage of the Cairngorms region available from the constellation is considered over a one week period both before and after the manoeuvres have been performed. **Figure 8** shows the total time in this one week period that a particular region has been viewed, with image (a) showing the results from the GOM constellation before manoeuvring and image (b) showing the results from the ROM constellation after manoeuvring. In the GOM case, the average time that the region is viewed is 2.8 minutes in a week, with the region of highest coverage receiving 3.4 minutes of coverage. After the manoeuvres have been carried out, this average coverage time increases to 4.3 minutes of coverage, with the best viewed regions receiving 8.4 minutes total coverage – more than twice that of the GOM case.

		ΔV , m/s	Manoeuvre Time, days	AoL after Manoeuvre, degs
Orbit Plane 1	Satellite 1	60	7.9	104.14
	Satellite 2	51	7.0	104.12
	Satellite 3	37	6.0	104.12
	Satellite 4	30	3.0	104.2
	Satellite 5	20	2.9	75.93
	Satellite 6	65	8.9	104.14
Orbit Plane 2	Satellite 7	72	9.2	104.12
	Satellite 8	70	8.2	104.14
	Satellite 9	63	7.2	104.16
	Satellite 10	48	6.2	104.16
	Satellite 11	39	4.3	104.35
	Satellite 12	35	4.1	76.04
Orbit Plane 3	Satellite 13	25	2.5	104.4
	Satellite 14	20	2.4	75.99
	Satellite 15	79	8.4	104.3
	Satellite 16	75	7.5	104.5
	Satellite 17	65	6.5	104.37
	Satellite 18	43	5.5	104.16
Orbit Plane 4	Satellite 19	41	6.7	104.18
	Satellite 20	34	4.7	104.14
	Satellite 21	32	4.6	75.85
	Satellite 22	87	9.5	76.09
	Satellite 23	58	8.7	104.2
	Satellite 24	52	7.7	104.13

Table 6: Possible Manoeuvres for all Satellites. Highlighted satellites are those selected to be manoeuvred.

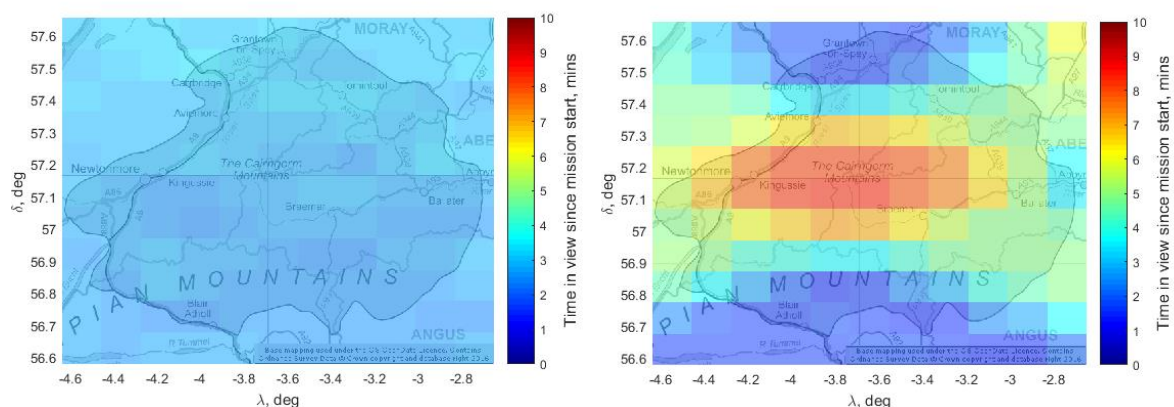


Figure 8: Total time that a region has been in view in a 1 week period (a) for the constellation before manoeuvring and (b) for the constellation after manoeuvring.

VI. Moving Target Case Study: Helicopter Communication

A. Introduction

The final case study considers providing communication and relay services to helicopters at a range of locations over time. In this case the locations follow a path from the UK to Svalbard, Norway, but the method is applicable to tracking any object whose locations at a given time are known in advance. Helicopters traditionally communicate directly with ground-based terminals, due to issues of rotor-blades disturbing the signal between a helicopter and a satellite. However, recent developments have made stable communications between helicopters and satellites possible [20]. This has the advantage of allowing communications away from ground terminal locations, such as over water. It also allows for enhanced communication when many helicopters are airborne in a small area, such as in response to a disaster, where air-ground radio congestion can be a problem [21]. Most proposed helicopter communications and tracking systems which make use of satellites select Iridium or geosynchronous spacecraft as their relay network. However, the use of dedicated small satellites could have advantages in certain situations as they would reduce the transmission power required by the helicopters due to their lower altitude and could provide dedicated, fast service in highly congested areas to, for example, prevent collisions and coordinate rescue efforts [21].

B. Method

This case study aims to find whether a dedicated small satellite could be used to provide communication and relay support to helicopters at a variety of locations over an 8 week period. In this study, the helicopters are known to be required at a variety of locations between the UK and Svalbard, Norway at one week intervals. The known future locations of the helicopters are given at one week intervals in *Table 8* and plotted in *Figure 9*.

In order to maximise communications opportunities with the helicopters, the satellite will target the known locations, hereafter referred to as ‘rendezvous locations’, at the earliest times the helicopters are known to be there, and will then remain for one week. It is thus decided that the satellite would manoeuvre once per week to end in a repeat ground track over the helicopter’s rendezvous location for that week. Once that week has passed, the satellite will move again to target the helicopters’ next rendezvous location, again ending in a repeated ground track over the area. The baseline orbit is selected to have an inclination of 78° to provide coverage of the full region of interest. The corresponding altitude for a repeating ground track is 545.285km. The full orbit parameters for this case are given in *Table 7*.

C. Results

For each manoeuvre to be performed, all possible manoeuvres which would finish at the correct altitude over the desired target are assessed using the analytical method described in Section III. As in the previous studies there is a trade-off for each manoeuvre between the time required for the manoeuvre and the ΔV that will be used. The distance to the target at flyover must also be considered. As such, the solutions are not unique. Two possible solutions were considered in this case; in Solution 1 the choice was made to first minimise manoeuvre time and then minimise ΔV , with no consideration given to the distance from the target at closest pass; in Solution 2 the manoeuvre choice was made to first minimise the manoeuvre time, then to minimise the distance to the target at flyover and finally to minimise ΔV . These solutions are presented in *Table 9* and *Table 10* respectively.

Parameter	Value	Units
Inclination	78	deg
Altitude	545.285	km
Instrument swath width	1000	km
Epoch	01 April 2006 00:00:00.0000	-
Right ascension of Greenwich at epoch	189.215	deg

Table 7: Helicopter Communication Case Study Initial Constellation Parameters.

Week	Longitude (degs)	Latitude (degs)
1	-3.63	55.02
2	-3.45	54.99
3	-3.41	54.97
4	-2.39	55.59
5	12.25	65.95
6	12.25	65.94
7	15.99	75.59
8	14.99	77.05

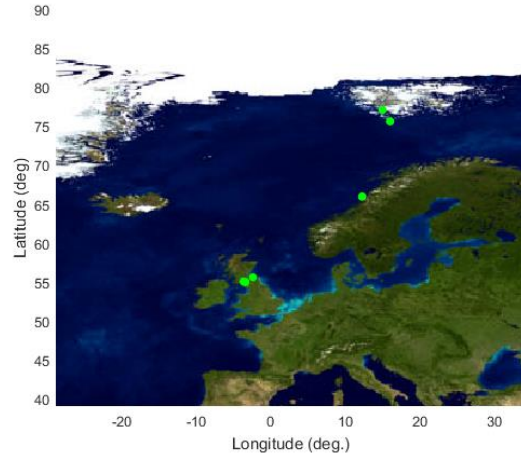


Table 8: Rendezvous location of helicopters at weekly intervals.

Figure 9: Helicopter known rendezvous locations (green).

Manoeuvre number	ΔV (m/s)	Time (days)	Distance to target (km)
1	15	3.5	44.5
2	2	0.99	48.5
3	1	0.99	47.1
4	5	1.98	46.9
5	23	3.96	47.7
6	1	0.65	46.2
7	1	0.72	34.7
8	31	5.01	49.99
Total:	79	18 out of 56 mission days spent maneuvering	

Table 9: Solution 1 manoeuvre descriptions.

Manoeuvre number	ΔV (m/s)	Time (days)	Distance to target (km)
1	21	3.5	0.5
2	3	0.99	4.4
3	1	0.99	0.2
4	10	0.99	16.1
5	33	3.31	42.8
6	6	0.65	48.3
7	7	0.72	33.5
8	50	5	39.7
Total:	131	16 out of 56 mission days spent maneuvering	

Table 10: Solution 2 manoeuvre descriptions.

Once the desired manoeuvres had been determined analytically, a numerical analysis of the scenario was run using a numerical simulator which propagates the position of the spacecraft using a set of modified equinoctial elements [22], using an explicit variable step size Runge Kutta (4,5) formula, the Dormand-Prince pair [23]. This was done for a non-manoeuving satellite in the orbit described in *Table 7*, as well as for a manoeuvring satellite following the manoeuvre strategy given by Solution 2 as shown in *Table 10*.

The results of this analysis for the non-manoeuving satellite are shown in *Figure 10*. The vertical black lines indicate the weeks and thus the times at which the point of interest changes in line with the change in rendezvous location as described in *Table 8*. From this it can be seen that the satellite will view the POIs 24 times over the eight week tracking period, however all of these views occur in the final two weeks of observation when the helicopters are at the northernmost point of the visible region. The results of the analysis for the manoeuvring satellite are shown in *Figure 11*. In this case the number of times the satellite will view the POIs increases to a total of 50 times, spread across the eight week tracking period, with a total ΔV of 131m/s used.

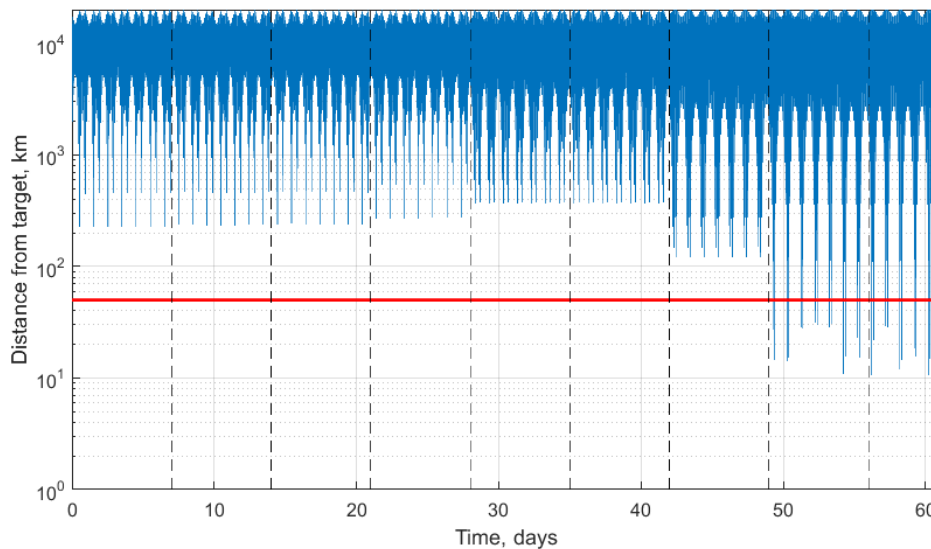


Figure 10: Distance from SSP to helicopter known rendezvous location plotted over time for non-manoeuving satellite. Dashed black lines indicate the weeks and hence the changes in target rendezvous location.

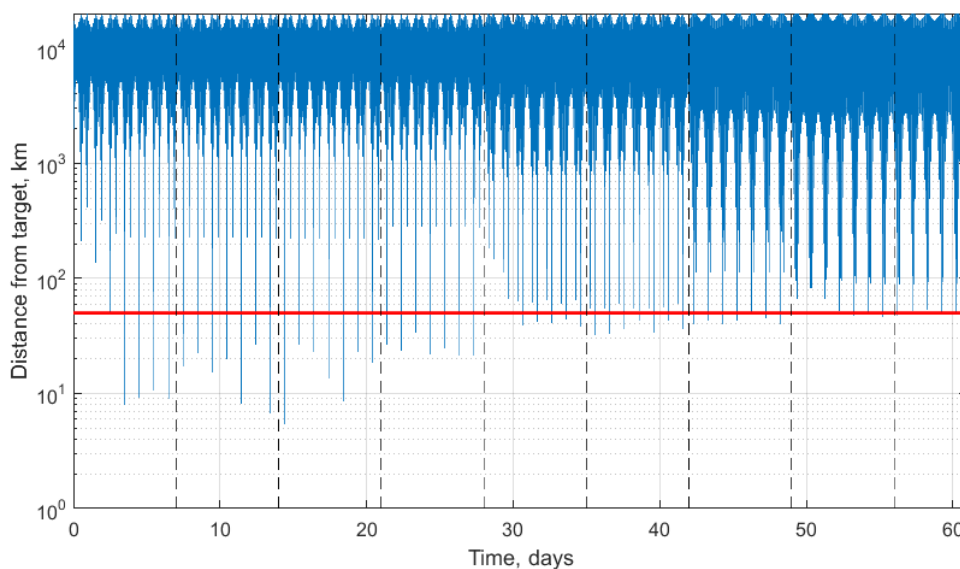


Figure 11: Distance from SSP to helicopter known rendezvous location plotted over time for manoeuvring satellite. Dashed black lines indicate the weeks and hence the changes in target rendezvous location.

VII. Conclusions

Manoeuvrable small satellites, and manoeuvrable constellations of small satellites, can be used to effectively carry out Earth observation missions requiring rapid response to changing mission requirements. Such responsive missions can provide significant improvements in the quantity of data collected and the frequency with which the data is obtained when compared with traditional, static satellite missions. The ability to manoeuvre can also enable unique missions, such as tracking of a moving target, which would not be possible with a static satellite or satellites. Responsive manoeuvrability can be realised using current nano-satellite technology; in particular the TILE electro-spray thruster developed at MIT is shown to provide sufficient thrust, operational time and ΔV to support a range of responsive mission scenarios.

Acknowledgements

This research was carried out during a research visit at the Massachusetts Institute of Technology, supported by a Fulbright-Schuman Student Grant administered by the Fulbright Commission for Educational Exchange. Ongoing research is supported by the EPSRC.

References

- [1] J. Bouwmeester and J. Guo, "Survey of worldwide pico-and nanosatellite missions, distributions and subsystem technology," *Acta Astronautica*, vol. 67, pp. 854-862, 2010.
- [2] C. Foster, H. Hallam, and J. Mason, "Orbit Determination and Differential-drag Control of Planet Labs Cubesat Constellations," presented at the AIAA Astrodynamics Specialist Conference, Vale, CO, 2015.
- [3] E. Hand, "CubeSat networks hasten shift to commercial weather data," ed: American Association for the Advancement of Science, 2017.
- [4] R. Welle, A. Utter, T. Rose, J. Fuller, K. Gates, B. Oakes, *et al.*, "A CubeSat-Based Optical Communication Network for Low Earth Orbit," presented at the 31st AIAA/USU Conference on Small Satellites, Utah, USA, 2017.
- [5] J. Tristanchó Martínez, "Implementation of a femto-satellite and a mini-launcher for the N Prize," Master in Aerospace Science & Technology, Applied Physics Department, Universitat Politècnica de Catalunya, 2010.
- [6] P. C. Lozano, "Less in Space," *American Scientist*, vol. 104, p. 270, 2016.
- [7] C. McGrath, E. Kerr, and M. Macdonald, "An analytical low-cost deployment strategy for satellite constellations" presented at the 13th Reinventing Space Conference, Oxford, 2015.
- [8] C. McGrath and M. Macdonald, "Design of a Reconfigurable Satellite Constellation," presented at the 66th International Astronautical Congress, Jerusalem, Israel, 2015.
- [9] C. N. McGrath and M. Macdonald, "Analytical Low-Thrust Satellite Maneuvers for Rapid Ground Target Revisit," in *AIAA SPACE 2016*, ed, 2016, p. 5294.
- [10] D. Krejci, F. Mier-Hicks, R. Thomas, T. Haag, and P. Lozano, "Emission Characteristics of Passively Fed Electro-spray Microthrusters with Propellant Reservoirs," *Journal of Spacecraft and Rockets*, 2017.
- [11] F. Mier-Hicks and P. C. Lozano, "Electro-spray Thrusters as Precise Attitude Control Actuators for Small Satellites," *Journal of Guidance, Control, and Dynamics*, 2016.
- [12] D. Krejci, F. Mier-Hicks, C. Fucetola, P. Lozano, A. H. Schouten, and F. Martel, "Design and Characterization of a Scalable ion Electro-spray Propulsion System," presented at the Joint Conference of 30th International Symposium on Space Technology and Science, 34th International Electric Propulsion Conference and 6th Nano-satellite Symposium, Hyogo-Kobe, Japan, 2015.
- [13] D. Krejci, F. Mier-Hicks, C. Fucetola, and P. Lozano, "High efficiency ionic liquid electro-spray propulsion for Nanosatellites," presented at the International Astronautical Congress, Guadalajara, Mexico, 2016.
- [14] D. A. Vallado and W. D. McClain, *Fundamentals of astrodynamics and applications* vol. 12: Springer Science & Business Media, 2001.
- [15] J. Castelví, E. Lancheros, A. Camps, and H. Park, "Feasibility of Nano-Satellites Constellations for AIS Decoding and Fire detection," in *FSS Workshop 2016 Proceedings*, 2016, pp. 1-6.
- [16] *GomSpace and AISTECH Sign a Binding Framework Delivery Agreement for the Supply of 100 Nanosatellite Platforms* Available: <https://gomspace.com/news/gomspace-and-aistech-sign-a-binding-framework.aspx>

- [17] R. S. Legge Jr, "Optimization and valuation of reconfigurable satellite constellations under uncertainty," Ph. D, Department of Aeronautics and Astronautics, Massachusetts Institute of Technology, 2014.
- [18] D. Mortari and M. P. Wilkins, "Flower constellation set theory. Part I: Compatibility and phasing," *IEEE Transactions on Aerospace and Electronic Systems*, vol. 44, 2008.
- [19] *Map Data from Google, Terrametrics, Grid Reference Finder.*
- [20] K. Yamamoto, Y. Ozaki, and H. Okuda, "Helicopter satellite communication system, helicopter-mounted communication apparatus, terrestrial station communication apparatus, communication method, and non-transitory computer-readable recording medium storing computer program," ed: Google Patents, 2016.
- [21] Y. Okuno, K. Kobayashi, and H. Ishii, "Development of a Helicopter Operations Management System for Disaster Relief Missions," *Journal of the American Helicopter Society*, vol. 61, pp. 1-9, 2016.
- [22] M. Walker, B. Ireland, and J. Owens, "A set modified equinoctial orbit elements," *Celestial mechanics*, vol. 36, pp. 409-419, 1985.
- [23] J. R. Dormand and P. J. Prince, "A family of embedded Runge-Kutta formulae," *Journal of computational and applied mathematics*, vol. 6, pp. 19-26, 1980.